Neurobiology of Disease 143 (2020) 105020

Contents lists available at ScienceDirect

Neurobiology of Disease

journal homepage: www.elsevier.com/locate/ynbdi

Disruption of endoplasmic reticulum-mitochondria tethering proteins in post-mortem Alzheimer's disease brain

Dawn H.W. Lau[1], Sebastien Paillusson[1], Naomi Hartopp, Huzefa Rupawala, Gábor M. Mórotz, Patricia Gomez-Suaga, Jenny Greig, Claire Troakes, Wendy Noble, Christopher C.J. Miller*

Department of Basic and Clinical Neuroscience, Institute of Psychiatry, Psychology and Neuroscience, King's College London, London SE5 9RX, UK

ARTICLE INFO

Keywords:
VAPB
PTPIP51
Endoplasmic reticulum
Mitochondria
Alzheimer's disease

ABSTRACT

Signaling between the endoplasmic reticulum (ER) and mitochondria regulates a number of key neuronal functions, many of which are perturbed in Alzheimer's disease. Moreover, damage to ER-mitochondria signaling is seen in cell and transgenic models of Alzheimer's disease. However, as yet there is little evidence that ER-mitochondria signaling is altered in human Alzheimer's disease brains. ER-mitochondria signaling is mediated by interactions between the integral ER protein VAPB and the outer mitochondrial membrane protein PTPIP51 which act to recruit and "tether" regions of ER to the mitochondrial surface. The VAPB-PTPIP51 tethers are now known to regulate a number of ER-mitochondria signaling functions including delivery of Ca^{2+} from ER stores to mitochondria, mitochondrial ATP production, autophagy and synaptic activity. Here we investigate the VAPB-PTPIP51 tethers in post-mortem control and Alzheimer's disease brains. Quantification of ER-mitochondria signaling proteins by immunoblotting revealed loss of VAPB and PTPIP51 in cortex but not cerebellum at end-stage Alzheimer's disease. Proximity ligation assays were used to quantify the VAPB-PTPIP51 interaction in temporal cortex pyramidal neurons and cerebellar Purkinje cell neurons in control, Braak stage III-IV (early/mid-dementia) and Braak stage VI (severe dementia) cases. Pyramidal neurons degenerate in Alzheimer's disease whereas Purkinje cells are less affected. These studies revealed that the VAPB-PTPIP51 tethers are disrupted in Braak stage III-IV pyramidal but not Purkinje cell neurons. Thus, we identify a new pathogenic event in post-mortem Alzheimer's disease brains. The implications of our findings for Alzheimer's disease mechanisms are discussed.

1. Introduction

Signal transduction processes enable eukaryotic cells to communicate with each other and to respond to physiological stimuli. An important component of this signaling involves communications between different organelles. Such crosstalk permits organelles to respond dynamically to changes in the cellular environment in an orchestrated manner (Cohen et al., 2018;Gordaliza-Alaguero et al., 2019). Communications between the endoplasmic reticulum (ER) and mitochondria represent a particularly important component of organelle signaling since this regulates a number of fundamental cellular processes. These include bioenergetics, Ca^{2+} homeostasis, lipid metabolism, mitochondrial biogenesis and trafficking, ER stress responses, autophagy and inflammation (Csordas et al., 2018;Krols et al., 2016;Lau et al., 2018;Paillusson et al., 2016;Rieusset, 2018;Rowland and Voeltz, 2012).

ER-mitochondria signaling is facilitated by close physical contacts between the two organelles such that up to 20% of the mitochondrial surface is tightly apposed to ER membranes. These regions of ER are termed mitochondria-associated ER membranes (MAM) (Csordas et al., 2018;Krols et al., 2016;Lau et al., 2018;Paillusson et al., 2016;Rieusset, 2018;Rowland and Voeltz, 2012). The mechanisms by which ER membranes are recruited to the mitochondrial surface are not fully understood but it is widely accepted that the process involves

Abbreviations: Aβ, amyloid-β;; ApoE4, ε4 allele of apolipoprotein E4;; ER, endoplasmic reticulum;; GSK3β, glycogen synthase kinase-3β;; IP3, inositol 1,4,5-trisphosphate; MAM, mitochondria associated ER membranes; MCU, mitochondrial Ca^{2+} uniporter; PDI, protein disulphide isomerase;; PLAs, proximity ligation assays;; PTPIP51, protein tyrosine phosphatase interacting protein-51;; RIPA, radioimmunoprecipitation assay;; VAPB, vesicle-associated membrane protein-associated protein B;; VDAC1, voltage dependent anion channel-1.

* Corresponding author.
E-mail address: chris.miller@kcl.ac.uk (C.C.J. Miller).

[1] These authors contributed equally to this work

https://doi.org/10.1016/j.nbd.2020.105020
Received 28 February 2020; Received in revised form 16 June 2020; Accepted 13 July 2020
Available online 17 July 2020

"tethering proteins" which act to scaffold the two organelles in close proximity. One tether involves an interaction between the integral ER protein, vesicle-associated membrane protein-associated protein B (VAPB) and the outer mitochondrial membrane protein, protein tyrosine phosphatase interacting protein-51 (PTPIP51) (De Vos et al., 2012;Stoica et al., 2014). The VAPB-PTPIP51 tethers are known to control a number of ER-mitochondria regulated functions including inositol 1,4,5-trisphosphate (IP3) receptor delivery of Ca^{2+} from ER stores to mitochondria, mitochondrial ATP production and autophagy (De Vos et al., 2012;Gomez-Suaga et al., 2017;Gomez-Suaga et al., 2019;Paillusson et al., 2017;Puri et al., 2019;Stoica et al., 2014;Stoica et al., 2016).

Many of the functions regulated by ER-mitochondria signaling are perturbed in Alzheimer's disease. These include mitochondrial biogenesis and ATP production, ER stress responses, Ca^{2+} signaling, lipid metabolism, autophagy, protein and organelle trafficking (especially axonal transport), and inflammatory responses (Area-Gomez et al., 2018;Krols et al., 2016;Paillusson et al., 2016). Moreover, synaptic activity has recently been shown to be regulated by ER-mitochondria signaling and synaptic damage is a prominent early feature of Alzheimer's disease (Gomez-Suaga et al., 2019;Hirabayashi et al., 2017). Such links have prompted investigations of ER-mitochondria contacts and signaling in Alzheimer's disease (Area-Gomez et al., 2018;Krols et al., 2016;Paillusson et al., 2016).

Mutations in the amyloid precursor protein (APP) and Presenilins (Presenilin-1 and -2) cause some familial forms of Alzheimer's disease (Schellenberg and Montine, 2012). APP is processed to produce amyloid-β (Aβ) that is deposited as a pathology in Alzheimer's disease and the Presenilins form part of the γ-secretase complex that cleaves APP to produce Aβ (Schellenberg and Montine, 2012). APP and the Presenilins all localise to ER-mitochondria contact sites, and MAM are a site of APP processing and Aβ production (Area-Gomez et al., 2009; Del Prete et al., 2017; Pera et al., 2017; Schreiner et al., 2015). Also both mutant Presenilins, APP and Aβ affect ER-mitochondria contacts and related functions (Area-Gomez et al., 2012; Hedskog et al., 2013; Martino Adami et al., 2019; Sepulveda-Falla et al., 2014; Zampese et al., 2011). Finally, the ε4 allele of apolipoprotein E (ApoE4) which is a major risk factor for Alzheimer's disease has been shown to affect MAM function (Tambini et al., 2015). Together, these studies support the notion that damage to the ER-mitochondria axis is part of the pathogenic process in Alzheimer's disease. Such findings also provide a plausible route for explaining many of the seemingly disparate pathological features of Alzheimer's disease (Area-Gomez et al., 2018; Krols et al., 2016; Paillusson et al., 2016).

However, to date these studies have focussed on cell and transgenic mouse models of Alzheimer's disease and as yet there is little evidence that ER-mitochondria contacts and signaling are affected in Alzheimer's disease brain. This represents a fundamental omission especially since APP and Presenilin transgenic mice only partially model Alzheimer's disease phenotypes (Puzzo et al., 2015;Sasaguri et al., 2017). Here, we address this issue by examining the ER-mitochondria tethering proteins VAPB and PTPIP51 in post-mortem Alzheimer's disease and control brains.

2. Materials and methods

2.1. Antibodies

The following primary antibodies were used in this study:

Rabbit and rat antibodies to VAPB and PTPIP51 were as described (De Vos et al., 2012). Rabbit anti-PTPIP51 antibody (Anti-RMDN3, HPA009975) and rabbit anti-Sigma-1 receptor (Anti-SIGMAR1, HPA018002) were from Atlas Antibodies. Mouse anti-protein disulphide isomerase (PDI) (RL77, MA3–018) was from Thermo Fisher Scientific. Rabbit anti-voltage-dependent anion channel-1 (VDAC1) (4866) and rabbit anti-mitochondrial Ca^{2+} uniporter (MCU) (D2Z3B, 14,997) were from Cell Signaling Technology. Rabbit anti IP3 receptor type-1 (117003) was from Synaptic Systems. Mouse anti-neuron specific enolase (NSE) (BBS/NC/VI-H14) was from Dako.

Table 1
Data for human post-mortem samples.

Group	Autopsy code	Sex	Age	Post-Mortem Delay (hrs)	ApoE allele	Braak stage
Control	BBN_14408	M	90	45	2/3	–
Control	BBN_24666	F	74	64	Unknown	II
Control	BBN_18401	M	82	47	3/4	I
Control	BBN_10250	F	92	9	2/3	II
Control	BBN_16291	M	82	18	3/3	–
Control	BBN_16242	F	90	50	3/3	II
Control	BBN_21801	M	68	60	Unknown	II
Control	BBN_22594	F	77	21	Unknown	–
Control	BBN_22991	F	73	27	Unknown	I
Control	BBN_18409	M	80	55	3/3	II-III
Control	BBN_10242	M	78	24	3/3	III
Control	BBN_24371	F	90	44	Unknown	II
Control	BBN_16218	F	84	34	2/3	I-II
Control	BBN_20040	F	80	22	3/4	II
Braak III-IV	BBN_9763	F	96	39	3/4	IV
Braak III-IV	BBN_9764	F	97	67.5	3/3	III-IV
Braak III-IV	BBN_002.28693	M	91	48	Unknown	IV
Braak III-IV	BBN_2931	F	92	19.5	3/3	III
Braak III-IV	BBN_15205	M	86	52.5	3/4	IV
Braak III-IV	BBN_002.28694	F	86	55.5	Unknown	IV
Braak III-IV	BBN_15210	M	82	28	4/4	IV
Braak III-IV	BBN_9887	F	92	29.5	3/3	IV
Braak III-IV	BBN_9977	F	83	22	3/3	IV
Braak III-IV	BBN_002.28871	F	95	47	Unknown	IV
Braak III-IV	BBN_9960	M	93	13.5	3/3	IV
Braak III-IV	BBN_24400	M	88	79	Unknown	III-IV
Braak III-IV	BBN_2459	M	98	53	Unknown	IV
Braak III-IV	BBN_002.29410	M	84	86	Unknown	IV
Braak VI	BBN_4191	M	66	41	3/3	VI
Braak VI	BBN_002.28677	F	93	49	Unknown	VI
Braak VI	BBN_002.28697	F	89	38.5	Unknown	VI
Braak VI	BBN_25019	F	73	30	Unknown	VI
Braak VI	BBN_15212	F	81	17.5	4/4	VI
Braak VI	BBN_4244	F	86	25	3/4	VI
Braak VI	BBN_23793	M	84	67	Unknown	VI
Braak VI	BBN_002.29056	F	69	73	Unknown	VI
Braak VI	BBN_002.29052	M	67	39.5	Unknown	VI
Braak VI	BBN_002.26678	M	86	38	Unknown	VI
Braak VI	BBN_24558	F	84	27	Unknown	VI
Braak VI	BBN_24382	F	79	31	Unknown	VI
Braak VI	BBN_24402	F	85	79	Unknown	VI
Braak VI	BBN_20124	F	81	20	3/4	VI

F = female; M = male.

2.2. Human tissue samples

Post-mortem human temporal cortex and cerebellum samples from control and clinically and pathologically confirmed cases of Alzheimer's disease were obtained from the Medical Research Council Neurodegenerative Diseases Brain Bank, King's College London. All tissue collection and processing were carried out under the regulations and licensing of the Human Tissue Authority, and in accordance with the UK Human Tissue Act, 2004. Post-mortem studies from some control, clinically non-demented individuals revealed early Braak stage pathologies. Details of the human cases are shown inTable 1; there were no significant differences in age or post-mortem delay between the Alzheimer's disease and control cases.

2.3. SDS-PAGE and immunoblotting

Frozen human brain tissues were processed for sodium dodecyl sulphate-polyacrylamide gel electrophoresis (SDS-PAGE) essentially as described previously with minor modifications (Morotz et al., 2019a;Morotz et al., 2019b). Briefly, tissues were prepared as 20%

homogenates in ice-cold radioimmunoprecipitation assay (RIPA) buffer (50 mM Tris-HCl, pH 7.4; 150 mM NaCl; 1 mM EDTA; 1% (*v*/v) Triton X-100; 0.5% (*w/v*) sodium deoxycholate; 0.1% (w/v) SDS) with protease and phosphatase inhibitor cocktails (Complete and PhosStop, Roche) using a Bio-Gen PRO200 rotor-stator homogeniser (Pro Scientific) for 20 s. Following homogenisation, each sample was sonicated three times for 3 s before being centrifuged at 13,000 x*g* for 20 min at 4 °C. Supernatants were collected and protein concentrations determined using a bicinchoninic acid protein concentration assay kit (Pierce) according to the manufacturer's instructions. Protein concentrations were adjusted to the same concentration in each sample by adding RIPA and SDS-PAGE sample buffers comprising 2% (w/v) SDS, 100 mM dithiothreitol, 10% (w/v) glycerol, 0.1% (w/v) bromophenol blue and protease inhibitors (Complete Roche) in 50 mM Tris-HCl pH 6.8 and heated to 96 °C for 10 min. Samples were stored at −80 °C.

SDS-PAGE and immunoblotting was performed as described previously (Morotz et al., 2019a;Morotz et al., 2019b). Briefly, samples were separated on Novex 4–12% Tris-Glycine Plus Midi Protein gels (Invitrogen) using the XCell4 Sureloc Midi-Cell system (Invitrogen). Separated proteins were transferred to BioTrace NT nitrocellulose membrane (0.2 μm pore size; Pall Corporation) using a Midi Trans-Blot electrophoretic transfer cell (Bio-Rad) for 2 h. Membranes were blocked with Odyssey blocking buffer, probed with primary antibodies in TBS containing 0.1% Tween 20 (wash buffer) and following washing, incubated with IRDye-conjugated secondary antibodies in wash buffer. Proteins were visualised using an Odyssey CLx near infrared imaging system (Li-Cor Biosciences). Protein signals were normalised to NSE signals.

2.4. Proximity ligations assays

VAPB-PTPIP51 PLAs were performed on 7 μm thick sections of paraffin wax embedded post-mortem human temporal cortex and cerebellum using rabbit VAPB and rat PTPIP51 antibodies with Duolink PLA reagents (Sigma). Donkey anti-rabbit in situ PLA probes were purchased directly; donkey anti-rat PLA probes were prepared using Duolink In Situ Probemaker kits. Signals were developed using Duolink In Situ Detection Brightfield kits. To do so, sections were dewaxed in xylene, rehydrated in graded alcohols and endogenous peroxidases blocked with hydrogen peroxide for 1 h at 20 °C. Antigen retrieval was conducted by microwave heating for 10 min in 10 mM citrate buffer pH 6.0. Sections were then incubated in Duolink block solution for 1 h at 37 °C and then with VAPB and PTPIP51 antibodies diluted in Duolink PLA diluent for 16 h at 4 °C. Following washing in Tris-HCl buffered saline containing 0.05% Tween 20, signals were developed using Duolink In Situ Detection Brightfield kit reagents essentially according to the manufacturer's instructions. Briefly, samples were incubated with Duolink ligation solutions and ligase for 1 h at 37 °C, washed and incubated with Duolink amplification reagents and polymerase for 2.5 h at 37 °C. Following further washes, PLA signals were developed by incubation with Duolink detection solution for 1 h and Duolink substrate solution for 20 min, both at 20 °C. Sections were then counterstained with haematoxylin, dehydrated in graded alcohols and xylene, and mounted in DPX mounting reagent. Controls involved omission of VAPB, PTPIP51 or both VAPB and PTPIP51 antibodies.

Sections were imaged using an Olympus VS120 slide scanner using an Olympus 40× UPlanSApo NA 0.95 lens and driven by Olympus L100 VS-ASW software. Cortical pyramidal and cerebellar Purkinje cells were identified by morphology and images analysed using Visiopharm 2018.4 Image Analyses software with an analyse package protocol created with Author Module.

2.5. Statistical analyses

Statistical analysis was performed using Excel (Microsoft Corporation) and Prism software (version 8; GraphPad Software Inc.). Statistical significance was determined as described in the figure legends.

3. Results

3.1. VAPB and PTPIP51 levels are reduced in post-mortem Alzheimer's disease cortex but not cerebellum

We first enquired whether expression of key ER-mitochondria signaling proteins might be altered in post-mortem Alzheimer's disease brain tissues. We studied VAPB and PTPIP51 since they function to tether ER domains with mitochondria, and a number of proteins involved in the delivery of Ca^{2+} from ER stores to mitochondria. This is because ER-mitochondria Ca^{2+} exchange controls several functions damaged in Alzheimer's disease such as mitochondrial ATP production, apoptosis and autophagy (Cardenas and Foskett, 2012;Csordas et al., 2018;Gomez-Suaga et al., 2017;Krols et al., 2016;Paillusson et al., 2016;Rowland and Voeltz, 2012). Delivery of Ca^{2+} from ER stores to mitochondria involves its release from ER located IP3 receptors and subsequent uptake into mitochondria via VDAC1 and the mitochondrial Ca^{2+} uniporter (MCU) (Csordas et al., 2018;Krols et al., 2016;Paillusson et al., 2016;Rowland and Voeltz, 2012). There are 3 subtypes of IP3 receptor (type-1, −2 and − 3) all of which function in delivery of Ca^{2+} to mitochondria (Bartok et al., 2019). However, they display differences in expression patterns within the nervous system; IP3 receptor type-1 is highly expressed in neurons in the cortex, hippocampus and cerebellum, IP3 receptor type-2 in mainly expressed in glia, and IP3 receptor type-3 is the major isoform in brain stem and spinal cord including motor neurons but is largely absent in cortex and hippocampus (De Smedt et al., 1994;Sharp et al., 1999;Watanabe et al., 2016). We therefore studied IP3 receptor type-1, VDAC1 and MCU levels. We also studied expression of the Sigma-1 receptor since it is a MAM protein that regulates several ER-mitochondria signaling functions (Hayashi, 2019;Su et al., 2016). Finally, we monitored expression of protein disulphide isomerase (PDI) which a major ER protein that is commonly used as a marker for changes to the ER in neurodegenerative diseases (Perri et al., 2015).

We quantified the levels of these proteins by immunoblotting of post-mortem temporal cortex and cerebellum in control, Braak stage III-IV (mid-dementia) and Braak stage VI (severe dementia) cases. Temporal cortex is a region of the brain that is most susceptible to Alzheimer's pathology whereas the cerebellum is the least affected brain region; analyses of the cerebellum is therefore often included for comparison and as an internal control in studies of Alzheimer's disease pathology (Andersen et al., 2012;Morotz et al., 2019a;Tavares et al., 2013;Tiwari et al., 2015). The levels of each protein were normalised to the levels of neuron specific enolase (NSE) as described by others (Kurbatskaya et al., 2016;Lau et al., 2016;Morotz et al., 2019a;Morotz et al., 2019b;Tiwari et al., 2015;Tiwari et al., 2016).

Compared to controls, VAPB, PTPIP51 and IP3 receptor type-1 levels were all significantly reduced in cortex in Braak stage VI cases (Fig. 1). The levels of VDAC1, MCU, the Sigma-1 receptor and PDI were unaffected (Fig. 1). By contrast, we detected no changes in expression of any of these proteins in cerebellum (Fig. 2). Thus, compared to control cases, the levels of VAPB, PTPIP51 and IP3 receptor type-1 are all reduced in Braak stage VI Alzheimer's disease cortex but not cerebellum.

We also enquired whether the loss of VAPB in Braak stage VI temporal cortex correlated with the reductions in PTPIP51 amounts in these cases. To do so, for each sample the NSE-normalised VAPB and PTPIP51 signals from immunoblots of control, Braak stage III-IV and Braak stage VI cases were correlated. These analyses revealed a highly significant overall correlation (Fig. 3A). On subgroup analyses, the control group showed positive correlation but the correlation was lost in both Braak stage III-IV and Braak stage VI groups (Fig. 3A). In a similar fashion, we also correlated VAPB levels with the ER protein PDI and PTPIP51 levels with the mitochondrial protein MCU. These analyses revealed a positive

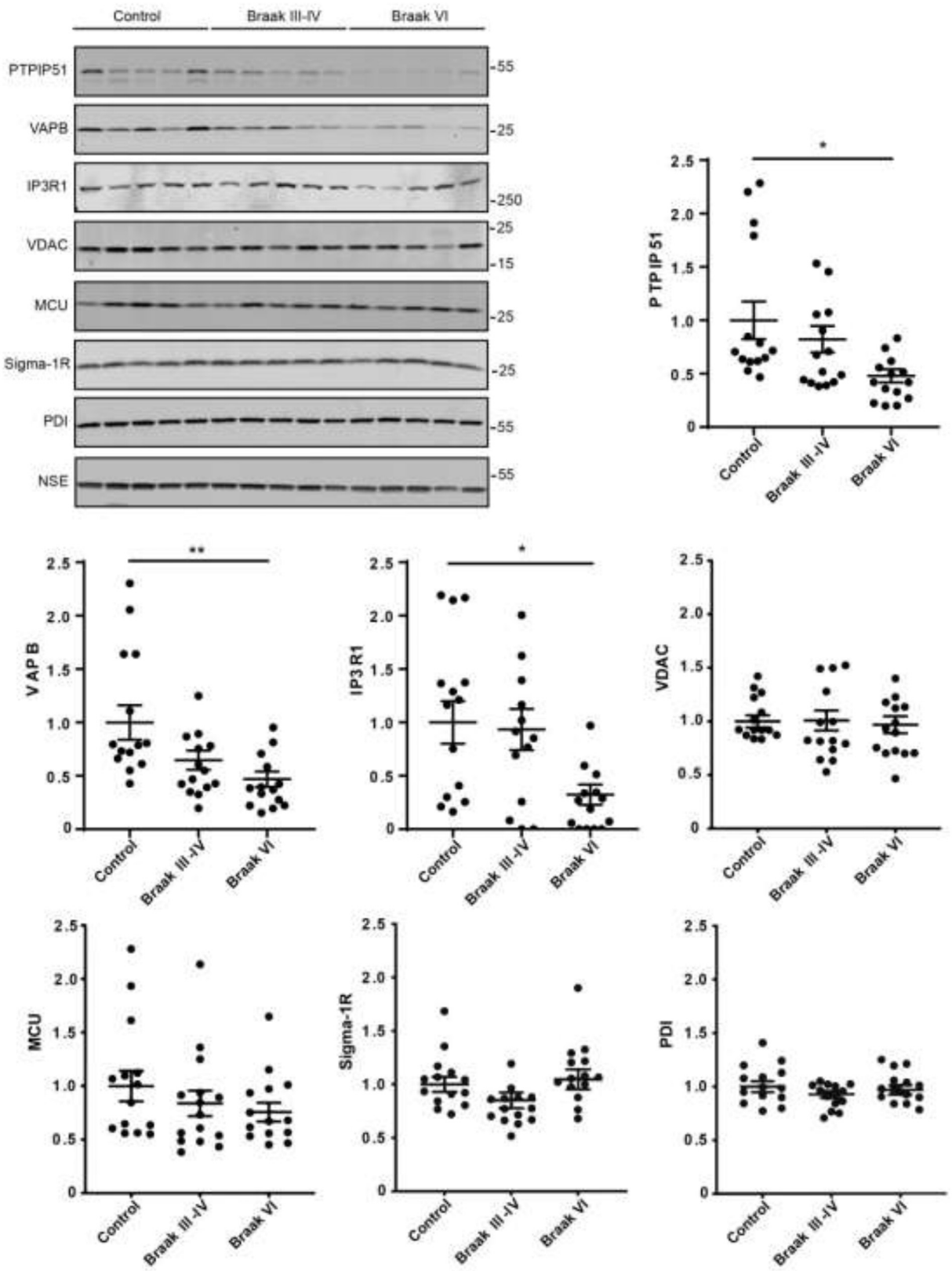

Fig. 1. Expression of MAM related proteins in post-mortem control and Alzheimer's disease temporal cortex. Representative immunoblots show levels of MAM related proteins in control, Braak stage III-IV and Braak stage VI brains. Graphs show quantification of MAM related protein levels in the different samples following normalisation to NSE levels in the same sample. Data were analysed by ANOVA and Tukey post hoc test; error bars are s.e.m., $*p < .05$ $**p < .01$.

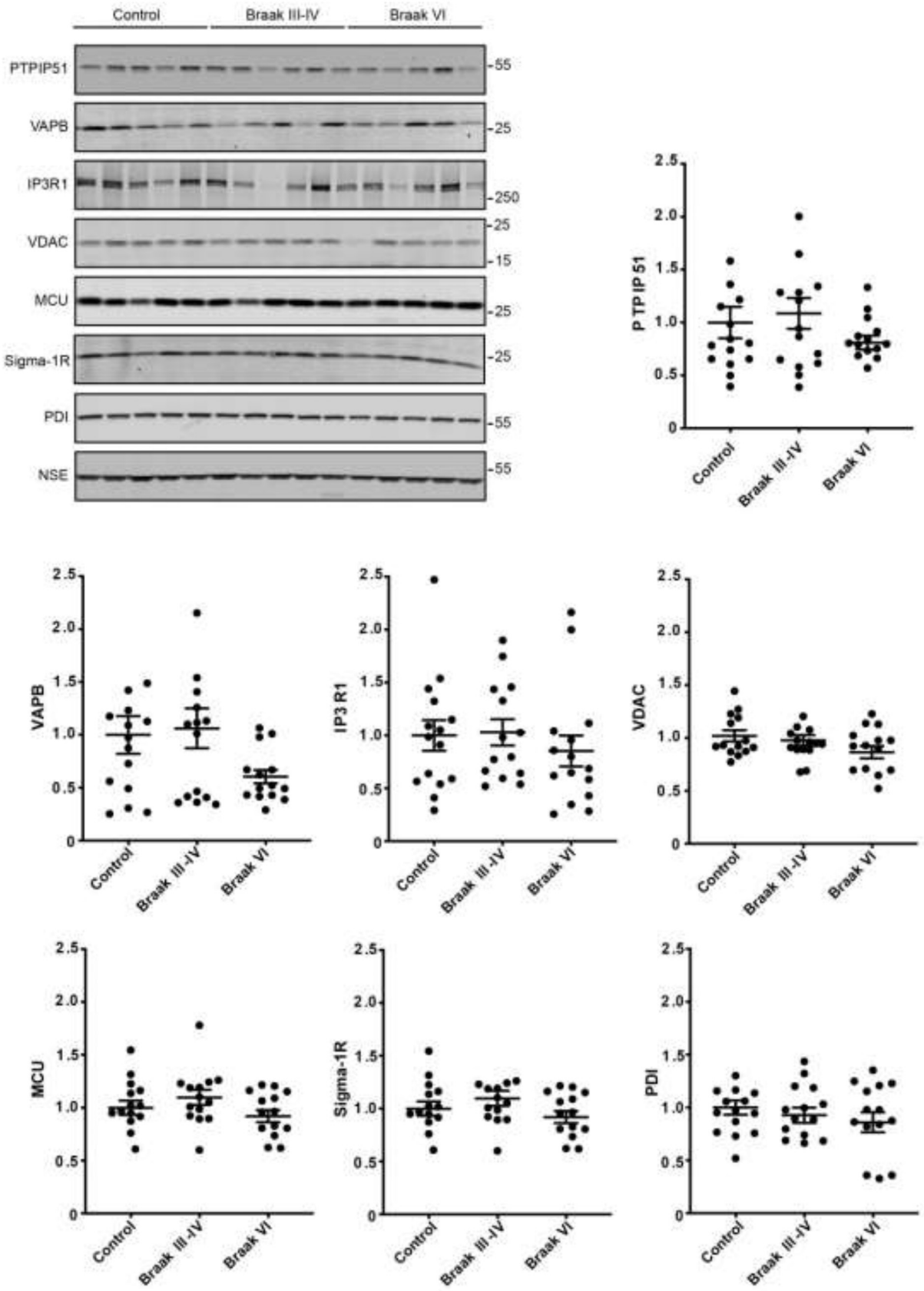

Fig. 2. Expression of MAM related proteins in post-mortem control and Alzheimer's disease cerebellum. Representative immunoblots show levels of MAM related proteins in control, Braak stage III-IV and Braak stage VI brains. Graphs show quantification of MAM related protein levels in the different samples following normalisation to NSE levels in the same sample. Data were analysed by ANOVA; error bars are s.e.m.

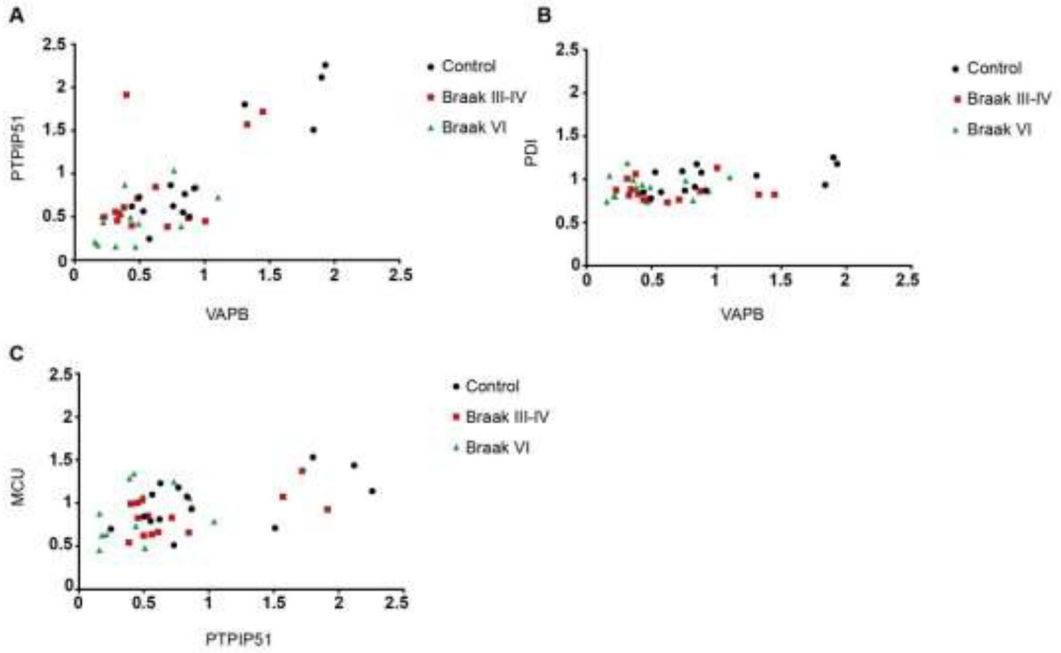

Fig. 3. Changes in levels of VAPB and PTPIP51 in temporal cortex correlate significantly but loss of VAPB does not correlate with ER PDI levels and loss of PTPIP51 does not correlate with mitochondrial MCU levels in Alzheimer's disease. NSE-normalised VAPB, PTPIP51, PDI and MCU signals from immunoblots were correlated by generating correlation coefficients and significance was established by non-parametric, two-tailed Spearman Rho tests. Graphs show normalised levels of VAPB and PTPIP51 (A), VAPB and PDI (B) and PTPIP51 and MCU (C) in the different samples. Each point in the graphs represents data from an individual case. Overall, VAPB and PTPIP51 levels displayed significant correlation ($r = 0.57, p < .0001$). However, whilst the control group showed positive correlation ($r = 0.68, p = .009$) the correlation was lost in the Alzheimer's groups (Braak stage III-IV, $r = 0.16, p = .59$; Braak stage VI $r = 0.42, p = .14$). A positive correlation between VAPB and PDI was detected in control cases ($r = 0.61, p = .02$) but this was lost in Braak stage III-IV ($r = -0.24, p = .41$) and Braak stage VI cases ($r = 0.05, p = .88$) cases. There was no correlation between PTPIP51 and MCU in control ($r = 0.52, p = .06$), Braak stage III-IV ($r = 0.29, p = .32$), or Braak stage VI cases ($r = 0.3$, p = .3) (Fig. 3C).

correlation between levels of VAPB and PDI in control cases but this was lost in Braak stage III-IV and Braak stage VI groups (Fig. 3B). There was no correlation between PTPIP51 and MCU in control, Braak stage III-IV, or Braak stage VI cases (Fig. 3C).

3.2. The VAPB-PTPIP51 interaction is disrupted in cortical pyramidal neurons but not cerebellar Purkinje cells in post-mortem Alzheimer's disease

We next quantified the VAPB-PTPIP51 interaction in cortical pyramidal neurons and in cerebellar Purkinje cells in the control and Alzheimer's disease tissues. Damage to cortical pyramidal neurons is a fundamental aspect of Alzheimer's disease whereas cerebellar Purkinje cells are relatively protected from such damage (Andersen et al., 2012;Mann, 1996). We quantified the VAPB-PTPIP51 interaction using in situ PLAs of sections of control and Alzheimer's disease cortex and cerebellum. The distances detected by PLAs are similar to those detected by resonance energy transfer between fluorophores (i.e. a maximum of 30 nm) and so these assays are suitable for quantifying ER-mitochondria contacts (Paillusson et al., 2016;Soderberg et al., 2006). Indeed, PLAs including ones for VAPB and PTPIP51 have already been used to quantify ER-mitochondria contacts and signaling (Bernard-Marissal et al., 2015;De Vos et al., 2012;Gomez-Suaga et al., 2019;Hedskog et al., 2013;Paillusson et al., 2017;Stoica et al., 2016).

To demonstrate the specificity of the PLAs, we first performed control experiments in which primary VAPB and/or PTPIP51 antibodies were omitted. Such omission produced none or only very few signals whereas inclusion of both antibodies generated large numbers of signals (Fig. 4). We then quantified the numbers of VAPB-PTPIP51 PLA signals in the control and Alzheimer's disease tissues and normalised the signal numbers/cell to the size of each cell so as to correct for any changes in neuron size in the Alzheimer's disease cases. Thus, any changes in PLA signals detected in the pyramidal and Purkinje cells cannot be the consequence of changes in cell size.

These studies revealed that compared to controls, VAPB-PTPIP51 PLA signal numbers/cell were significantly reduced in Braak stage III-IV but not Braak stage VI pyramidal cells (Fig. 5). By contrast, we detected no changes in VAPB-PTPIP51 PLA signal numbers in Purkinje cells between the control and Alzheimer's disease cases (Fig. 6).

4. Discussion

A number of studies support the notion that ER-mitochondria signaling is damaged in Alzheimer's disease (Area-Gomez et al., 2012;Del Prete et al., 2017;Hedskog et al., 2013;Leal et al., 2018;Martino Adami et al., 2019;Pera et al., 2017;Schreiner et al., 2015;Sepulveda-Falla et al., 2014;Tambini et al., 2015;Zampese et al., 2011). However, these studies largely focused on experimental models and to date, there is little evidence that ER-mitochondria contacts and signaling are altered in Alzheimer's disease brain. Here, we utilised PLAs to study the VAPB-PTPIP51 interaction in post-mortem temporal cortex and cerebellum in control, Braak stage III-IV and Braak stage VI Alzheimer's disease cases.

Our studies involved 14 control, 14 Braak stage III-IV and 14 Braak stage VI Alzheimer's disease cases and we analysed between 95 and 270 pyramidal neurons per case. For comparison, we also quantified the VAPB-PTPIP51 interaction in cerebellar Purkinje cells in the same cases since these neurons are relatively less affected in Alzheimer's disease (Andersen et al., 2012;Mann, 1996). Compared to controls, we detected a significant decrease in VAPB-PTPIP51 PLA signals in cortical pyramidal cells in the Braak stage III-IV but not Braak stage VI cases; we detected no changes in PLA signals in Purkinje cells. These findings suggest that the VAPB-PTPIP51 tethers are disrupted in pyramidal but not Purkinje cells in Braak stage III-IV but not late-stage Alzheimer's disease.

We also detected fewer VAPB-PTPIP51 PLA signals in the control

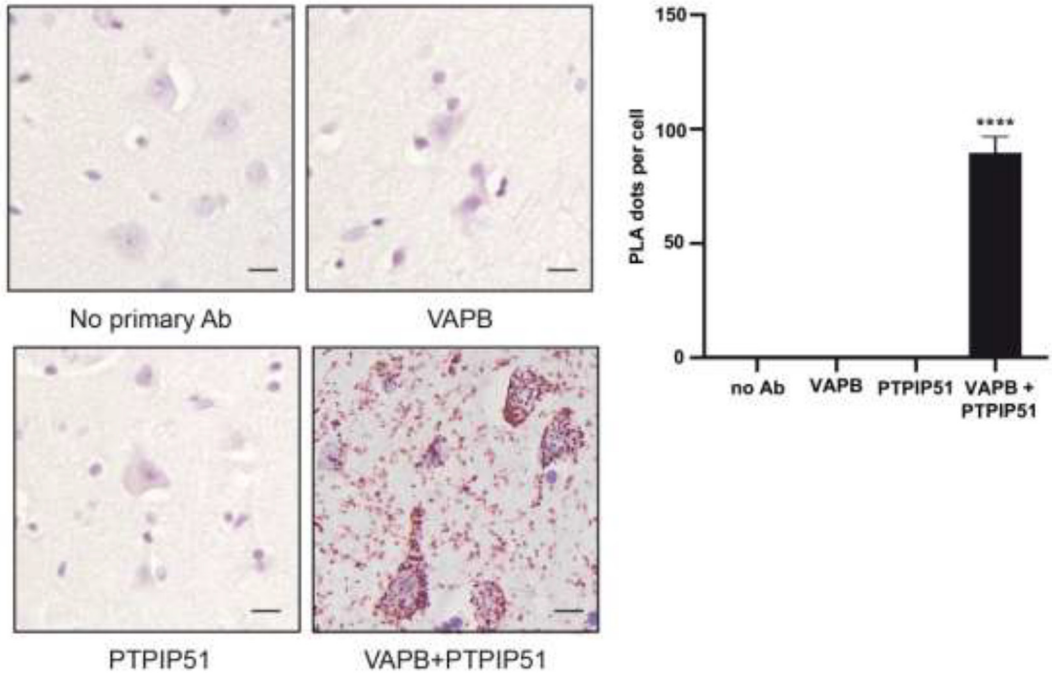

Fig. 4. Control experiments demonstrating the specificity of VAPB-PTPIP51 PLAs on human post-mortem temporal cortex brain sections. Controls involved omission of VAPB, PTPIP51, or both VAPB and PTPIP51 primary antibodies (no primary Ab). Graph shows PLA signals per cell (temporal cortex pyramidal neurons) in the different experiments. Data were analysed by ANOVA and Tukey post hoc test.N = 26–30 cells per treatment, error bars are s.e.m., ****$p < .0001$. Scale bar = 25 μm.

Purkinje cell neurons compared to control pyramidal cells. These results suggest differences in ER-mitochondria contacts and signaling between these two neuronal cell types. Indeed, Purkinje cell have unique Ca^{2+}handling mechanisms and there are marked differences in mitochondrial makeup between different neuronal cell types (Fecher et al., 2019;Meera et al., 2016).

The mechanisms that underlie breaking of the VAPB-PTPIP51 tethers in the Braak stage III-IV pyramidal cells are not clear. The expression levels of VAPB and PTPIP51 have been shown to affect ER-mitochondria contacts and linked functions; loss of VAPB and/or PTPIP51 disrupts tethering whereas overexpression increases tethering (De Vos et al., 2012;Gomez-Suaga et al., 2017;Gomez-Suaga et al., 2019;Paillusson et al., 2017;Stoica et al., 2014). We detected decreased levels of both VAPB and PTPIP51 in cortex but not cerebellum in the Braak stage VI cases. However, the PLA data revealed breaking of the VAPB-PTPIP51 tethers in Braak stage III-IV but not Braak stage VI tissues. Thus, disruption of VAPB-PTPIP51 tethering may not be due to changes in expression of these proteins. Indeed, the reduced levels of VAPB and PTPIP51 that we detect in total Braak stage VI temporal cortex do not mean that the levels of these proteins are altered in individually affected pyramidal neurons. Also, the absence of any changes in VAPB-PTPIP51 PLA signals in the Braak stage VI pyramidal cells cases may be linked to a resistance of this sub-population of neurons to neurodegeneration since they represent some of the remaining cells in late-stage disease.

An alternative possibility is that the disruption is linked to activation of glycogen synthase kinase-3β (GSK3β). GSK3β is a favoured kinase for phosphorylating Tau in Alzheimer's disease and GSK3β has been shown to inhibit the VAPB-PTPIP51 interaction and reduce ER-mitochondria contacts (Lovestone et al., 1994; Stoica et al., 2014; Stoica et al., 2016). However, the activity of GSK3β in post-mortem human Alzheimer's disease tissues has proved to be controversial. For example, increased tyrosine-216 phosphorylation (which is required for activity) but no change in serine-9 phosphorylation (which inhibits activity) has been reported in Alzheimer's disease (Leroy et al., 2007). By contrast, another study reported no change in tyrosine-216 phosphorylation but an increase in inhibitory serine-9 phosphorylation in Alzheimer's disease (Swatton et al., 2004). Finally, a third study reported increased serine-9 phosphorylated GSK3β in affected neurons in Alzheimer's disease indicating reduced activity (Ferrer et al., 2002). Such studies have led to the conclusion that “it is technically difficult, if not impossible, to measure (GSK3β sic) enzymatic activity in post-mortem brain tissue” (Hooper et al., 2008). One route to address this issue in human samples in future studies would be to correlate levels of GSK3β activity with changes in the VAPB-PTPIP51 interaction in neurons derived from induced pluripotent stem cells from Alzheimer's disease patients carrying familial pathogenic mutations; some studies of such neurons reveal activation of GSK3β via altered serine-9 phosphorylation (Israel et al., 2012).

Recently, ER-mitochondria contacts have been analysed by electron microscopy in human brain biopsy cases from idiopathic normal pressure hydrocephalus patients. Of the 14 cases analysed in this study, three patients presented comorbidity with dementia; one with Alzheimer's disease, one with Alzheimer's disease and vascular dementia, and one with Lewy body dementia (Leal et al., 2018). Clearly, firm conclusions on any changes in ER-mitochondria contacts in Alzheimer's disease and any linkage of such changes to Braak staging cannot be made from these studies, especially since the primary disease was not dementia. Also, these studies did not discriminate between ER-mitochondria contacts in neurons or glia (Leal et al., 2018). However, these biopsy studies are important in that they formally reveal the presence of ER-mitochondria contacts similar to those found in other human tissues and mammalian organisms.

Other studies of ER-mitochondria contacts and signaling in models of Alzheimer's disease have provided conflicting data (Area-Gomez et al., 2012;Del Prete et al., 2017;Hedskog et al., 2013;Martino Adami et al., 2019;Pera et al., 2017;Schreiner et al., 2015;Sepulveda-Falla et al., 2014;Tambini et al., 2015;Zampese et al., 2011). For example, it is not clear whether mutant Presenilin-1 and/or − 2 affect ER-mitochondria signaling nor whether these mutants increase or decrease

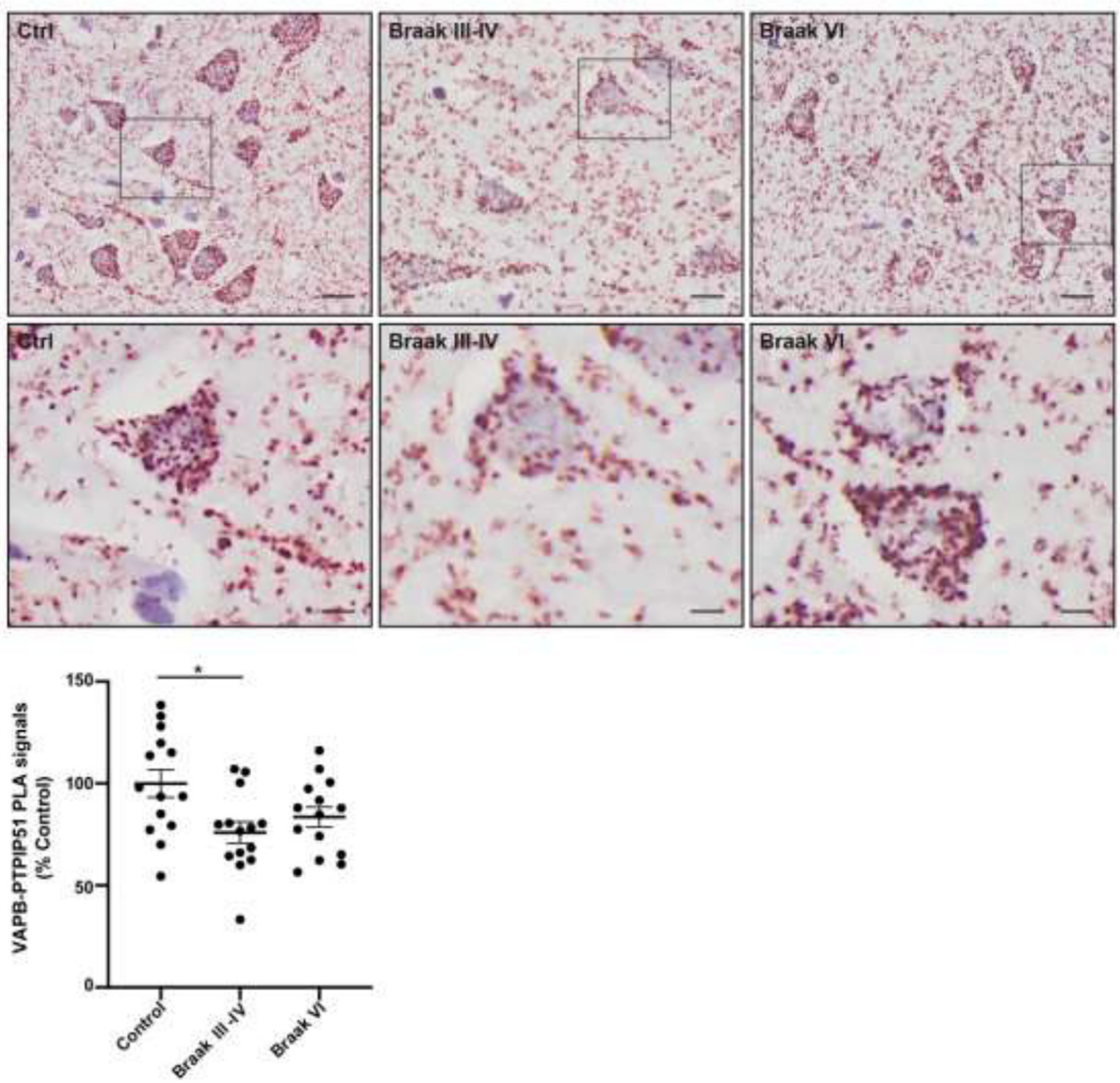

Fig. 5. The VAPB-PTPIP51 interaction is reduced in temporal cortex pyramidal neurons in Braak stage III-IV but not Braak stage VI Alzheimer's disease. Representative images of VAPB-PTPIP51 PLAs in pyramidal cells of control, Braak stage III-IV and Braak stage VI Alzheimer's disease brains. Top panel shows low magnification and bottom panel shows zoom of boxed area at higher magnification. Graph shows mean number of VAPB-PTPIP51 PLA signals per pyramidal neuron for each case. VAPB-PTPIP51 signal numbers were normalised to the size of each cell so as to correct for any changes in neurons size in the Alzheimer's disease cases. The numbers of neurons analysed per case were:N = 103–265 (control cases), N = 95–240 (Braak III-IV cases), N = 100–270 (Braak VI cases). N = 14 cases for each. Data were analysed by Welch's ANOVA and Dunnett post hoc test; Error bars are s.e.m., *p = .0136. Scale bars; 25 μm (top panel) and 7 μm (bottom panel).

contacts (Area-Gomez et al., 2012;Sepulveda-Falla et al., 2014;Zampese et al., 2011). Likewise, there is conflicting data on the effects of APP and Aβ on ER-mitochondria contacts and signaling (Del Prete et al., 2017; Hedskog et al., 2013; Martino Adami et al., 2019). The reasons for these differing results are not clear but may be due to the different experimental systems, assays and methods of analyses used to quantify ER-mitochondria contacts and signaling. There is also evidence that different expression levels of neurodegenerative disease linked mutant proteins can generate opposing effects on ER-mitochondria signaling in experimental systems (Cali et al., 2019). Finally, although the apolipoprotein E4 (ApoE4) allele (which is a major risk factor for Alzheimer's disease) has been shown to upregulate MAM activity, treatment of cells with ApoE4 does not significantly alter ER and mitochondria co-localisation compared to ApoE3 (Tambini et al., 2015).

Here, we present the first study of the VAPB-PTPIP51 ER-mitochondria tethers in post-mortem Alzheimer's disease brain and reveal that the tethers are disrupted in Braak stage III-IV pyramidal cells i.e. relatively early in the disease process. The VAPB-PTPIP51 tethers are now known to regulate a number of fundamental physiological processes that are likewise damaged relatively early in Alzheimer's disease. These include Ca^{2+}homeostasis, energy metabolism, autophagy and synaptic activity (De Vos et al., 2012;Gomez-Suaga et al., 2017;Gomez-Suaga et al., 2019;Paillusson et al., 2017;Paillusson et al., 2016). Disruption of the VAPB-PTPIP51 tethers may therefore contribute to such damage.

Both mitochondria and MAM proteins can be isolated biochemically and such purifications permit analyses of protein content in these fractions; such analyses revealed that VAPB is a MAM protein and that PTPIP51 is an outer mitochondrial membrane protein (De Vos et al., 2012). It would therefore be interesting to compare MAM protein content in human control and Alzheimer's disease brains. However, robust analyses of such purified MAM proteins requires fresh (non-frozen) tissues (Wieckowski et al., 2009), ideally with short post-mortem times. Such studies are therefore beyond the scope of this

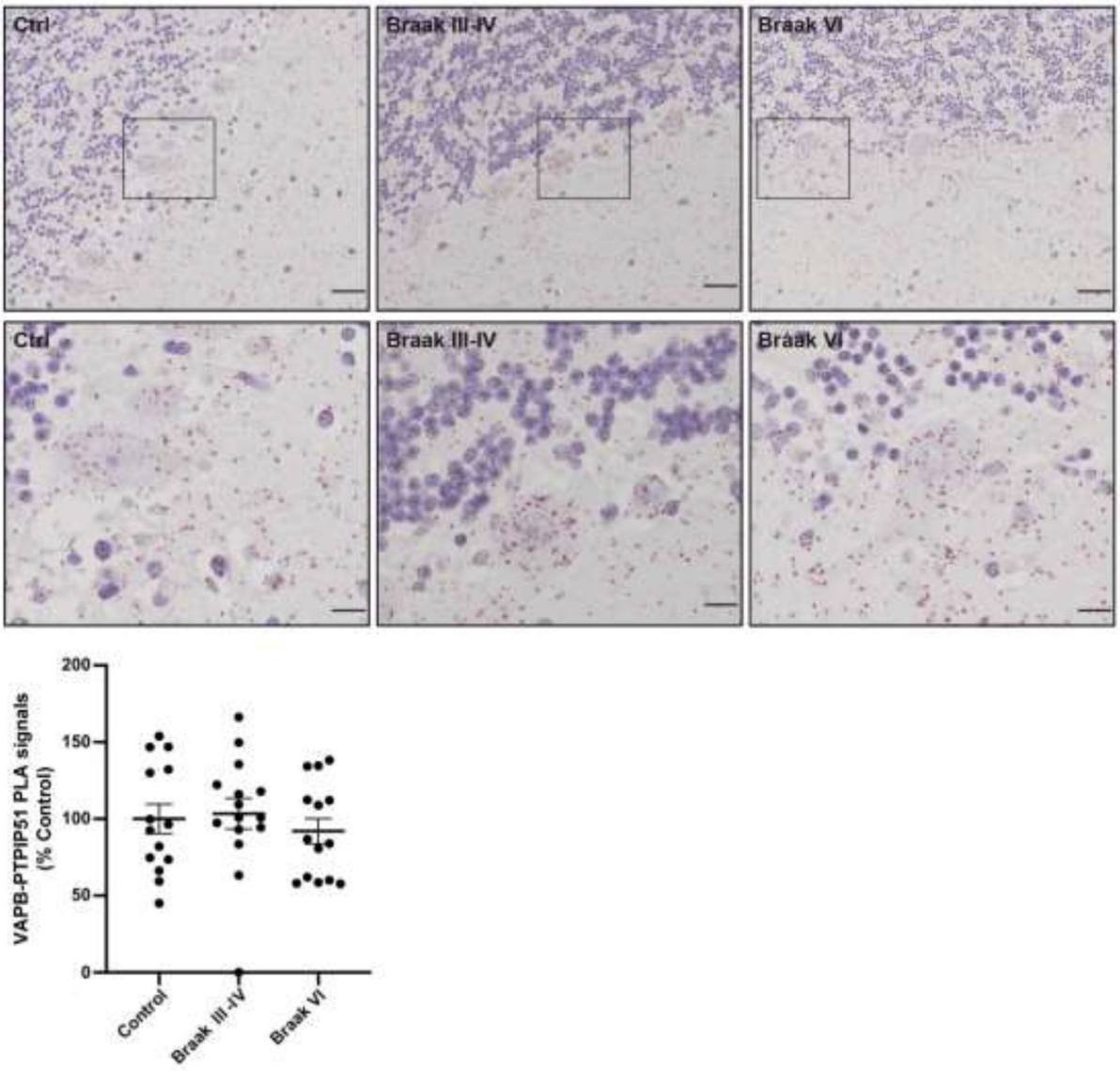

Fig. 6. The VAPB-PTPIP51 interaction is not altered in cerebellar Purkinje cell neurons in Alzheimer's disease. Representative images of VAPB-PTPIP51 PLAs in Purkinje cell neurons of control, Braak stage III-IV and Braak stage VI Alzheimer's disease brains. Top panel shows low magnification and bottom panel shows zoom of boxed area at higher magnification. Graph show mean number of VAPB-PTPIP51 PLA signals per Purkinje cell neuron for each case. VAPB-PTPIP51 signal numbers were normalised to the size of each cell so as to correct for any changes in neurons size. The numbers of neurons analysed per case were:*N* = 99–199 (control cases), N = 100–199 (Braak III-IV cases), N = 100–199 (Braak VI cases). N = 14 cases for each. Data were analysed by Welch's ANOVA; Error bars are s.e.m. Scale bars; 25 μm (top panel) and 7 μm (bottom panel).

study. Interestingly however, a recent investigation examined inflammatory microRNAs in MAM in Alzheimer's disease brain (Wang et al., 2020). For these studies, fresh human tissues (less than 4 h post-mortem) were collected and utilised. Similar analyses of MAM proteins would be of value in future studies.

In conclusion, we show that the levels of the key ER-mitochondria tethering proteins VAPB and PTPIP51 are reduced in temporal cortex but not cerebellum in late stage Alzheimer's disease. Using PLAs, we also show that the VAPB-PTPIP51 tethers are disrupted in affected pyramidal neurons in post-mortem Alzheimer's disease cortex and that this disruption occurs at a relatively early stage of disease. Our results reveal a new pathological phenotype in Alzheimer's disease.

Authors' contributions

CCJM, WN and DHWL planned the study. DHWL, SP, NH, GMM, PG-S and HR performed experiments and analysed data. CT provided input for post-mortem tissues and provided expertise. All authors edited the manuscript.

Declaration of Competing Interest

The authors declare they have no competing interests.

Acknowledgements

We thank Sashika Selvackadunco (King's College London) for technical assistance. This work was supported by grants from Alzheimer's Research UK (ARUK-PG2014–5 and ARUK-PG2017B-3), the UK Medical Research Council (MR/R022666/1), the Alzheimer's Society (AlzSoc-287), Biotechnology and Biological Sciences Research Council (BB/L09299/1) and Motor Neurone Disease Association (Gomez-Suaga/Oct17/967/799).

References

Andersen, K., et al., 2012. Stereological quantification of the cerebellum in patients with Alzheimer's disease. Neurobiol. Aging 33 (197), e11–e20.

Area-Gomez, E., et al., 2009. Presenilins are enriched in endoplasmic reticulum membranes associated with mitochondria. Am. J. Pathol. 175, 1810–1816.

Area-Gomez, E., et al., 2012. Upregulated function of mitochondria-associated ER membranes in Alzheimer disease. EMBO J. 31, 4106–4123.

Area-Gomez, E., et al., 2018. A key role for MAM in mediating mitochondrial dysfunction in Alzheimer disease. Cell Death Dis. 9, 335.

Bartok, A., et al., 2019. IP3 receptor isoforms differently regulate ER-mitochondrial contacts and local calcium transfer. Nat. Commun. 10, 3726.

Bernard-Marissal, N., et al., 2015. Dysfunction in endoplasmic reticulum-mitochondria crosstalk underlies SIGMAR1 loss of function mediated motor neuron degeneration. Brain. 138, 875–890.

Cali, T., et al., 2019. splitGFP technology reveals dose-dependent ER-mitochondria Interface modulation by alpha-Synuclein A53T and A30P mutants. Cells 8.

Cardenas, C., Foskett, J.K., 2012. Mitochondrial ca(2+) signals in autophagy. Cell Calcium 52, 44–51.

Cohen, S., et al., 2018. Interacting organelles. Curr. Opin. Cell Biol. 53, 84–91.

Csordas, G., et al., 2018. Endoplasmic reticular-mitochondrial Contactology: structure and signaling functions. Trends Cell Biol. 28, 523–540.

De Smedt, H., et al., 1994. Determination of relative amounts of inositol trisphosphate receptor mRNA isoforms by ratio polymerase chain reaction. J. Biol. Chem. 269, 21691–21698.

De Vos, K.J., et al., 2012. VAPB interacts with the mitochondrial protein PTPIP51 to regulate calcium homeostasis. Hum. Mol. Genet. 21, 1299–1311.

Del Prete, D., et al., 2017. Localization and processing of the amyloid-beta protein precursor in mitochondria-associated membranes. J. Alzheimers Dis. 55, 1549–1570.

Fecher, C., et al., 2019. Cell-type-specific profiling of brain mitochondria reveals functional and molecular diversity. Nat. Neurosci. 22, 1731–1742.

Ferrer, I., et al., 2002. Glycogen synthase kinase-3 is associated with neuronal and glial hyperphosphorylated tau deposits in Alzheimer's disease, Pick's disease, progressive supranuclear palsy and corticobasal degeneration. Acta Neuropathol. 104, 583–591.

Gomez-Suaga, P., et al., 2017. The ER-mitochondria tethering complex VAPB-PTPIP51 regulates autophagy. Curr. Biol. 27, 371–385.

Gomez-Suaga, P., et al., 2019. The VAPB-PTPIP51 endoplasmic reticulum-mitochondria tethering proteins are present in neuronal synapses and regulate synaptic activity. Acta Neuropathol. Commun. 7, 35.

Gordaliza-Alaguero, I., et al., 2019. Metabolic implications of organelle-mitochondria communication. EMBO Rep. 20 (9), e47928.

Hayashi, T., 2019. The Sigma-1 receptor in cellular stress signaling. Front. Neurosci. 13, 733.

Hedskog, L., et al., 2013. Modulation of the endoplasmic reticulum-mitochondria interface in Alzheimer's disease and related models. Proc. Natl. Acad. Sci. U. S. A. 110, 7916–7921.

Hirabayashi, Y., et al., 2017. ER-mitochondria tethering by PDZD8 regulates Ca2+ dynamics in mammalian neurons. Science. 358, 623–630.

Hooper, C., et al., 2008. The GSK3 hypothesis of Alzheimer's disease. J. Neurochem. 104, 1433–1439.

Israel, M.A., et al., 2012. Probing sporadic and familial Alzheimer's disease using induced pluripotent stem cells. Nature. 482, 216–220.

Krols, M., et al., 2016. Mitochondria-associated membranes as hubs for neurodegeneration. Acta Neuropathol. 131, 505–523.

Kurbatskaya, K., et al., 2016. Upregulation of calpain activity precedes tau phosphorylation and loss of synaptic proteins in Alzheimer's disease brain. Acta Neuropathol. Commun. 4, 34.

Lau, D.H., et al., 2016. Critical residues involved in tau binding to fyn: implications for tau phosphorylation in Alzheimer's disease. Acta Neuropathol. Commun. 4, 49.

Lau, D.H.W., et al., 2018. Disruption of ER-mitochondria signalling in fronto-temporal dementia and related amyotrophic lateral sclerosis. Cell Death Dis. 9, 327.

Leal, N.S., et al., 2018. Alterations in mitochondria-endoplasmic reticulum connectivity in human brain biopsies from idiopathic normal pressure hydrocephalus patients. Acta Neuropathol Commun. 6, 102.

Leroy, K., et al., 2007. Increased level of active GSK-3beta in Alzheimer's disease and accumulation in argyrophilic grains and in neurones at different stages of neurofibrillary degeneration. Neuropathol. Appl. Neurobiol. 33, 43–55.

Lovestone, S., et al., 1994. Alzheimer's disease-like phosphorylation of the microtubule-associated protein tau by glycogen synthase kinase-3 in transfected mammalian cells. Curr. Biol. 4, 1077–1086.

Mann, D.M., 1996. Pyramidal nerve cell loss in Alzheimer's disease. Neurodegeneration. 5, 423–427.

Martino Adami, P.V., et al., 2019. Perturbed mitochondria-ER contacts in live neurons modelling Alzheimer's disease amyloid pathology. J. Cell Sci. 132 (20), jcs229906.

Meera, P., et al., 2016. Cellular and circuit mechanisms underlying spinocerebellar ataxias. J. Physiol. 594, 4653–4660.

Morotz, G.M., et al., 2019a. LMTK2 binds to kinesin light chains to mediate anterograde axonal transport of cdk5/p35 and LMTK2 levels are reduced in Alzheimer's disease brains. Acta Neuropathol. Commun. 7, 73.

Morotz, G.M., et al., 2019b. Kinesin light chain-1 serine-460 phosphorylation is altered in Alzheimer's disease and regulates axonal transport and processing of the amyloid precursor protein. Acta Neuropathol. Commun. 7, 200.

Paillusson, S., et al., 2016. There's something wrong with my MAM; the ER-mitochondria axis and neurodegenerative diseases. Trends Neurosci. 39, 146–157.

Paillusson, S., et al., 2017. Alpha-Synuclein binds to the ER-mitochondria tethering protein VAPB to disrupt Ca2+ homeostasis and mitochondrial ATP production. Acta Neuropathol. 134, 129–149.

Pera, M., et al., 2017. Increased localization of APP-C99 in mitochondria-associated ER membranes causes mitochondrial dysfunction in Alzheimer disease. EMBO J. 26, 3356–3371.

Perri, E.R., et al., 2015. The unfolded protein response and the role of protein disulfide isomerase in neurodegeneration. Front. Cell Dev. Biol. 3, 80.

Puri, R., et al., 2019. Mul1 restrains Parkin-mediated mitophagy in mature neurons by maintaining ER-mitochondrial contacts. Nat. Commun. 10, 3645.

Puzzo, D., et al., 2015. Rodent models for Alzheimer's disease drug discovery. Expert Opin. Drug Discovery 10, 703–711.

Rieusset, J., 2018. Mitochondria-associated membranes (MAMs): an emerging platform connecting energy and immune sensing to metabolic flexibility. Biochem. Biophys. Res. Commun. 500, 35–44.

Rowland, A.A., Voeltz, G.K., 2012. Endoplasmic reticulum-mitochondria contacts: function of the junction. Nat. Rev. Mol. Cell Biol. 13, 607–625.

Sasaguri, H., et al., 2017. APP mouse models for Alzheimer's disease preclinical studies. EMBO J. 36, 2473–2487.

Schellenberg, G.D., Montine, T.J., 2012. The genetics and neuropathology of Alzheimer's disease. Acta Neuropathol. 124, 305–323.

Schreiner, B., et al., 2015. Amyloid-beta peptides are generated in mitochondria-associated endoplasmic reticulum membranes. J. Alzheimers Dis. 43, 369–374.

Sepulveda-Falla, D., et al., 2014. Familial Alzheimer's disease-associated presenilin-1 alters cerebellar activity and calcium homeostasis. J. Clin. Invest. 124, 1552–1567.

Sharp, A.H., et al., 1999. Differential cellular expression of isoforms of inositol 1,4,5-triphosphate receptors in neurons and glia in brain. J. Comp. Neurol. 406, 207–220.

Soderberg, O., et al., 2006. Direct observation of individual endogenous protein complexes in situ by proximity ligation. Nat. Methods 3, 995–1000.

Stoica, R., et al., 2014. ER-mitochondria associations are regulated by the VAPB-PTPIP51 interaction and are disrupted by ALS/FTD-associated TDP-43. Nat. Commun. 5, 3996.

Stoica, R., et al., 2016. ALS/FTD-associated FUS activates GSK-3beta to disrupt the VAPB-PTPIP51 interaction and ER-mitochondria associations. EMBO Rep. 17, 1326–1342.

Su, T.P., et al., 2016. The Sigma-1 receptor as a pluripotent modulator in living systems. Trends Pharmacol. Sci. 37, 262–278.

Swatton, J.E., et al., 2004. Increased MAP kinase activity in Alzheimer's and down syndrome but not in schizophrenia human brain. Eur. J. Neurosci. 19, 2711–2719.

Tambini, M.D., et al., 2015. ApoE4 upregulates the activity of mitochondria-associated ER membranes. EMBO Rep. 17, 27–36.

Tavares, I.A., et al., 2013. Prostate-derived sterile 20-like kinases (PSKs/TAOKs) phosphorylate tau protein and are activated in tangle-bearing neurons in Alzheimer disease. J. Biol. Chem. 288, 15418–15429.

Tiwari, S.S., et al., 2015. Evidence that the presynaptic vesicle protein CSPalpha is a key player in synaptic degeneration and protection in Alzheimer's disease. Mol. Brain. 8, 6.

Tiwari, S.S., et al., 2016. Alzheimer-related decrease in CYFIP2 links amyloid production to tau hyperphosphorylation and memory loss. Brain. 139, 2751–2765.

Wang, W.X., et al., 2020. The mitochondria-associated ER membranes are novel subcellular locations enriched for inflammatory-responsive MicroRNAs. Mol. Neurobiol. 57, 2996–3013.

Watanabe, S., et al., 2016. Mitochondria-associated membrane collapse is a common pathomechanism in SIGMAR1- and SOD1-linked ALS. EMBO Mol. Med. 8, 1421–1437.

Wieckowski, M.R., et al., 2009. Isolation of mitochondria-associated membranes and mitochondria from animal tissues and cells. Nat. Protoc. 4, 1582–1590.

Zampese, E., et al., 2011. Presenilin 2 modulates endoplasmic reticulum (ER)-mitochondria interactions and Ca2+ cross-talk. Proc. Natl. Acad. Sci. U. S. A. 108, 2777–2782.